Clinical Interventions in Aging

Dovepress
open access to scientific and medical research

Open Access Full Text Article

ORIGINAL RESEARCH

Protective effect of Anwulignan against D-galactose-induced hepatic injury through activating p38 MAPK–Nrf2–HO-1 pathway in mice

This article was published in the following Dove Press journal:
Clinical Interventions in Aging

Jiaqi Gao[1,*]
Zepeng Yu[1,*]
Shu Jing[2]
Weihai Jiang[2]
Cong Liu[1]
Chunyan Yu[1]
Jinghui Sun[1]
Chunmei Wang[1]
Jianguang Chen[1]
He Li[1]

[1]Department of Pharmacology, College of Pharmacy, Beihua University, Jilin City, People's Republic of China; [2]Affiliated Hospital of Beihua University, Jilin City, People's Republic of China

*These authors contributed equally to this work

Background: Liver aging is a significant risk factor for chronic liver diseases. Oxidative stress has been considered as a conjoint pathological mechanism for the initiation and progression of liver aging. It has been reported that D-galactose (D-gal)-induced hepatic injury is an experimental model well established closely similar to morphological and functional features of liver aging. Schisandra sphenanthera Rehd. et Wils (S. sphenanthera, Schisandraceae), as a famous tradi-tional Chinese medicine, has been used for thousands of years in China to treat various disorders, including liver dysfunctions. This study was aimed to understand whether Anwulignan, one of the monomeric compounds in the lignans from S. sphenanthera, could improve the hepatic injury induced by D-gal in mice and to examine the possible mechanisms.

Methods: ICR mice were used to produce hepatic injury by 220 mg kg-1 D-gal subcutaneously once daily for 42 days. The effects of oral Anwulignan on liver index; serial AST and ALT levels; histological changes; SOD, GSH-Px, MDA, and 8-OHdG in the liver and peripheral blood; expression of p38 mitogen-activated protein kinase (MAPK), Nrf2, and HO-1 in the liver; and HepG2 cell viability, and decrease caspase-3 contents in liver were examined.

Results: Anwulignan could significantly increase the liver index, lower aspartate aminotransferase (AST) and alanine aminotransferase (ALT) levels in the peripheral blood, elevate superoxide dismutase (SOD) and glutathione peroxidase (GSH-Px) activities, and decrease malonaldehyde (MDA) and 8-hydroxy-2-deoxyguanosine (8-OHdG) contents in the peripheral blood and liver. Furthermore, Anwulignan could upregulate the expression of p38 mitogen-activated protein kinase (MAPK), Nrf2, and HO-1 in the liver, increase the HepG2 cell viability, and decrease caspase-3 contents in liver.

Conclusion: Anwulignan has protective effects against the hepatic injury induced by D-gal, which may be related to its antioxidant capacity through activating p38 MAPK–Nrf2–HO-1 pathway, increases the injured cell viability, and decreases the caspase-3 contents in liver.

Keywords: Schisandra, antioxidant capacity, caspase-3

Introduction

Liver aging is a significant risk factor for chronic liver diseases.[1,2] ROS are involved in the aging process and result mainly from nonenzymatic processes in the liver.[3] Therefore, the inhibition and blockade of oxidative stress should be promising therapeutic strategies for liver aging. Studies have shown that overload of D-galactose (D-gal) can increase the production of ROS, resulting in oxidative stress that can attack essential cell constituents, induce lipid peroxidation, damage the membranes of cells and organelles in liver, cause the swelling and necrosis of hepatocytes, and ultimately result in hepatic injury.[4,5] *Schisandra sphenanthera*, the dried ripe fruit of *S. sphenanthera* Rehd. et Wils, is used as a restorative, tonic, and nutrition in many countries.[6,7] Studies have found that it can treat hepatic injury through its hepatoprotective and antioxidant activities and *Wuzhi*

Correspondence: Jianguang Chen; He Li
Department of Pharmacology, College of Pharmacy, Beihua University, No 3999 Binjiang East Road, Fengman, Jilin City 132013, Jilin, People's Republic of China
Tel +86 432 6460 8278
Email chenjg@beihua.edu.cn; yitonglh@126.com

submit your manuscript | www.dovepress.com
Dovepress
http://dx.doi.org/10.2147/CIA.S173838

capsule contains an ethanol extract from *S. sphenanthera* and has been often used as a hepar-protecting and enzyme-decreasing drug in clinical practice.[8–13] Anwuligan is a monomeric compound isolated from *S. sphenanthera*[14] and is also one of the main components of *Wuzhi* capsule.[14–16] However, there is no study to reveal its antioxidant and protective effects on hepatic injury. Therefore, we designed this study to understand whether Anwulignan can improve the D-gal-induced hepatic injury and to investigate the possible mechanisms.

Materials and methods

Experimental animals, materials, and reagents

Clean grade healthy male Institute of Cancer Research mice, weighing 20±2 g, were provided by the Experimental Animal Research Center of Jilin University, and the experimental animal breeding license number was SCXK (Ji): 2017-0005. The mice were raised in separate cages and in a diurnal cycle of 12 hours:12 hours and on a standard laboratory feed and water ad libitum. The animal experiments were approved by the Institutional Animal Care and Use Committee (IACUC) of Beihua University. All of the experimental procedures were performed in accordance with the Guide for the Care and Use of Laboratory Animals (China).

Anwulignan (Chengdu Pufei De Biotech Co., Ltd., Chengdu, China), sodium carboxymethyl cellulose (AR) (Shandong Weifang Lite Composite Materials Co., Ltd., Weifang, China), Twain-20 (AR) (Tianjin Yungtay Reagent Company, Tianjin, China), D-gal (Sigma-Aldrich Co., St Louis, MO, USA), polyvinylidene fluoride (PVDF) film, HCl-Tris, 30% acrylamide, *N*,*N*,*N*′,*N*′-tetramethylethylenediamine (TEMED), ammonium persulfate, Tris hydroxy methyl aminomethan, glycine, and diethypyrocarbonate (DEPC) water (Beijing Dinguo Reagent Company, Beijing, China), aspartate aminotransferase (AST) kit, alanine aminotransferase (ALT) kit, 8-hydroxy-2-deoxyguanosine (8-OHdG) kit, glutathione peroxidase (GSH-Px) kit, superoxide dismutase (SOD) kit, malonaldehyde (MDA) kit, and DNA marker (Nanjing Jiancheng Bioengineering Institute, Nangjing, China), skim milk powder (BD Company, San Francisco, CA, USA), rabbit anti-p38 mitogen-activated protein kinase (MAPK) antibody, rabbit anti-phospho-p38 MAPK (T180/Y182) antibody, rabbit anti-Nrf2 antibody (EPR1390Y), and rabbit anti-HO-1 antibody (EP1808Y) (Abcam, San Francisco, CA, USA), rabbit anti-caspase-3 (0206130101) (ABclonal Biotechnology Co., Ltd., Wuhan, China), caspase-3 ELISA kit (MLBIO Biotechnology Co., Ltd., Shanghai, China); electrochemiluminescence (ECL) color liquid (Biyuntian Biological Products Co., Ltd., Beijing, China), RNA extraction kit (Vazyme Biotech Co., Ltd., Nangjing, China), broad spectrum protein marker (Beijing Soledao Technology Co., Ltd., Beijing, China), agarose (Shanghai Genview Company Co., Ltd., Shanghai, China), and HepG2 cells (American Type Culture Collection [ATCC], Manassas, VA, USA) were used. DMEM and other culture reagents were obtained from HyClone (Logan, UT, USA).

Animal treatments

ICR mice were randomly divided into five groups, such as control group (CON, distilled water orally and normal saline subcutaneously), model group (MOD, distilled water orally and 220 mg kg^{-1} D-gal subcutaneously), and three Anwulignan groups (1, 2, and 4 mg kg^{-1} of Anwulignan orally, respectively, and 220 mg kg^{-1} D-gal subcutaneously for all three groups), 15 mice in each group, and administered once daily for 42 days. The mice were anesthetized with ether 30 minutes after the last administration, and blood was collected by removing eyeballs. The serum was separated by centrifugation and stored at −80°C, and the livers of mice in all the groups were removed, weighed, and then stored at −80°C for use.

Detection of liver index

The mice and their livers were weighed 30 minutes after the last administration, and the liver index was calculated according to the following equation:

$$\text{Liver index} = \frac{\text{Weight of liver (g)}}{\text{Body weight (g)}} \times 100\%$$

Detection of AST and ALT levels in the peripheral blood

Mice from each group were selected and sacrificed 30 minutes after the last administration, then their peripheral serum samples were collected, and the levels of AST and ALT were detected according to the kit instructions.

Histological analysis

Three mice in random were anesthetized with ether and sacrificed by decapitation, and the liver samples were taken. The liver was fixed with 10% formalin, embedded with paraffin, and cut into slices of 5–10 μm thick. The slices were stained by hematoxylin-eosin staining (HE) staining and observed under an OLYMPUS optical microscope for examining the pathological changes.

Detection of SOD, GSH-Px, MDA, and 8-OHdG in the liver and peripheral blood

Twelve mice were randomly selected from each group and were sacrificed 30 minutes after the last administration, and

then their liver tissue and peripheral serum samples were collected. An equal amount of liver was homogenized, and the supernatants were used for the detection.[17] The protein contents of the supernatants were detected following the modified method described in the previous study.[17] The activities of SOD and GSH-Px and the level of lipid peroxidation product MDA were determined by using commercial kits. The level of caspase-3 in liver was determined by using enzyme-linked immunosorbent assay kit. In addition, the genomic DNA of liver was first isolated using the Genomic DNA Mini Preparation Kit and, then, the level of 8-OHdG was detected according to the manufacturer's protocol of a mouse 8-OHdG enzyme-linked immunosorbent assay kit.

Reverse transcription PCR

The liver samples of three mice from each group were taken 30 minutes after the last administration, the total cellular RNA in the samples was extracted according to the kit instructions, and the cDNA was synthesized by following the instructions of reverse transcription reaction kit. The reverse transcription PCR amplification reaction was performed according to the kit instructions, each of the gene sequence number was found in Genebank, the primers were designed by primer software six and synthesized by Beijing Dingguo Changsheng Biotechnology Company, Beijing, China, and β-actin was the reference gene. All the primers are shown in Table 1.

The amplification conditions were predenaturation at 94°C for 3 minutes, denaturation at 94°C for 30 seconds and annealing for 30 seconds (annealing temperature: 55°C for p38 MAPK, 58°C for Nrf2 and HO-1, and 63.5°C for β-actin), and extension at 72°C for 30 seconds, with 30 cycles, then extension at 72°C for 7 minutes, and finally, save at 4°C. The gel electrophoresis on 10 μL PCR products was carried out, the results were observed and photographed by the gel imaging system (Tanon 1600 gel Image system; Shanghai Tianneng Technology Co., Ltd., Shanghai, China), the density of the photographs was scanned by the gel imaging system, and the OD values of p38 MAPK, Nrf2, and HO-1 were used to express the relative amount of mRNA.

Western blot

Liver samples of three mice from each group were taken 3 minutes after the last administration. The samples were added with the lysis buffer on the ice for cracking for 1 hour and then centrifuged at 16,009.2× *g* to obtain the supernatant. The tissue protein concentration in the supernatant was determined by bicinchoninic acid (BCA) method, and 10% SDS-PAGE gel electrophoresis was used to isolate Nrf2, HO-1, β-actin, p38 MAPK, and phosphorylation of p38 MAPK (p-p38 MAPK). The proteins were transferred onto PVDF membrane for 2 hours, and the membrane was rinsed with Tris buffer saline Tween (TBST) for 5 minutes and then blocked with the blocking buffer (TBST buffer containing 5% skim milk powder) for 1 hour. After the incubation at room temperature, the blocking buffer was discarded. The first antibodies of Nrf2 (1:1,000), HO-1 (1:1,000), β-actin (1:1,000), p38 MAPK (1:1,000), and p-p38 MAPK (1:1,000) were added onto the membrane, respectively, which was incubated at 4°C overnight and then washed with TBST five times, 5 minutes each time; the second antibody (HRP Goat Anti-Rabbit IgG (H+L), 1:2,000) were added onto the membrane, which was incubated for 2 hours and then washed five times with TBST, 5 minutes each time, and finally, ECL color solution was added onto the membrane for its development.

HepG2 cell culture and treatments

HepG2 cells were cultured in DMEM supplemented with 10% FBS, 100 IU mL^{-1} penicillin, and 0.1 μg mL^{-1} streptomycin. The cells were incubated in humidified atmosphere of 5% CO_2 at 37°C, passaged according to the recommended procedures of ATCC, used for experiments from the logarithmic phase of growth, and seeded into 96-well plates (1×10^4 cells per well, 100 μL). Cells were exposed to D-gal (at 18.75, 37.5, 75, 150, and 300 mM) or Anwulignan (at 0.625, 1.25, 2.5, 5, and 10 μg mL^{-1}) for 24 hours for determining the concentrations of D-gal and Anwulignan. The final concentrations were 75 mM for D-gal to produce the liver injury model, and 0.625, 1.25, and 2.5 μg mL^{-1} for Anwulignan. All cells were cultured for 24 hours.

Determination of HepG2 cell viability

HepG2 cell viability was determined by MTT assay method. Briefly, MTT (5 mg mL^{-1}, 20 μL per well) was added into the cell-seeded 96-well plates, and the cells were incubated at 37°C for 4 hours. Then, the solutions were removed

Table 1 Primer sequence

Name	Forward	Reverse
p38 MAPK (203 bp)	5′ CCGAACGATACCAGAACC 3′	5′ ATCCAACAGACCAATCACAT 3′
Nrf2 (276 bp)	5′ GTGCTCCTATGCGTGAAT 3′	5′ TACCTCTCCTGCGTATATCT 3′
HO-1 (295 bp)	5′ TCAGGTGTCCAGAGAAGG 3′	5′ CAGGTAGCGGGTATATGC 3′
β-Actin (182 bp)	5′ CCCATCTACGAGGGCTAT 3′	5′ TGTCACGCACGATTTCC 3′

and DMSO (150 µL per well) was added into the wells. The absorbance was measured at 490 nm using a 96-well plate reader. Cell viability was calculated as follows: cell viability (100%) = absorbance of Anwulignan-treated group/absorbance of CON group ×100%.

Statistical analysis

The experimental data were expressed as mean ± SD. The statistical analysis was performed by one-way ANOVA followed by the Tukey's test for multiple comparisons using the SPSS software (SPSS 19.0; IBM Corporation, Armonk, NY, USA). Differences were considered to be significant when *P*-value was <0.05.

Results

Effects of Anwulignan on the liver functions of D-gal-treated mice

Liver index, AST, and ALT are important indicators for evaluating liver function.[18,19] In order to observe the effect of Anwulignan on the liver function of D-gal-treated mice, we observed those three indicators. The results showed that the liver indexes (Figure 1A), in the MOD group, were significantly reduced in comparison to the CON group ($P<0.01$). Whereas, in comparison to the MOD group, the liver indexes were increased significantly in 4 mg kg^{-1} Anwulignan group ($P<0.05$), those in 1 and 2 mg kg^{-1} Anwulignan groups showed no significant changes ($P>0.05$).

The effects of Anwulignan on AST and ALT in the serum of mice were also examined. As shown in Figure 1B and C, in comparison to the CON group, the serum ALT and AST levels of the mice in the MOD group were significantly increased ($P<0.01$). However, in comparison to the MOD group, the serum AST and ALT levels of the mice were significantly reduced in 2 and 4 mg kg^{-1} Anwulignan groups ($P<0.05$ and $P<0.01$, respectively), while they were not significantly changed in 1 mg kg^{-1} Anwulignan group ($P>0.05$).

Effects of Anwulignan on pathological changes in the liver tissue of D-gal-treated mice

In order to evaluate the effect of Anwulignan on the morphology of hepatocytes, the hepatocytes were stained by HE

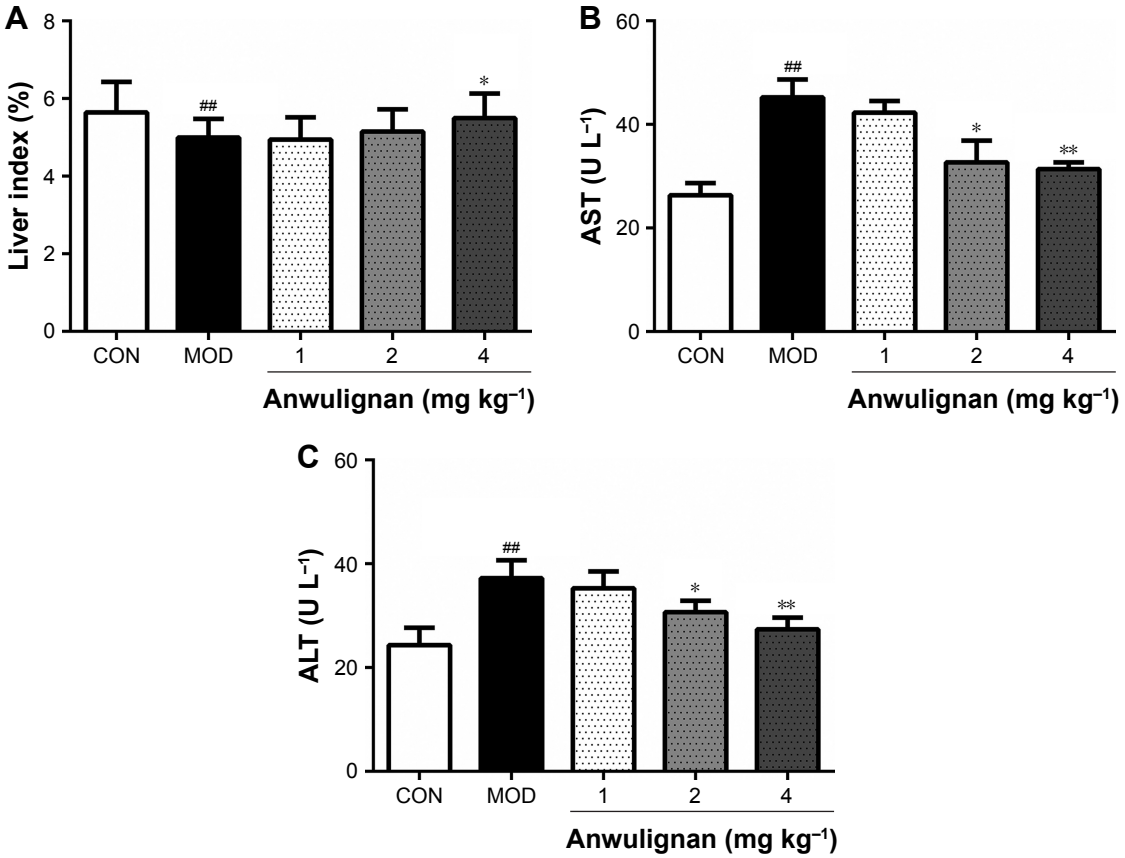

Figure 1 Effects of Anwulignan on the liver function of mice (mean ± SD, n=15).
Notes: (**A**) Effect of Anwulignan on the liver index. (**B**) Effect of Anwulignan on the AST level in the peripheral blood. (**C**) Effect of Anwulignan on the ALT level in the peripheral blood. ##$P<0.01$, compared with the control group; *$P<0.05$, compared with the model group; **$P<0.01$, compared with the model group.
Abbreviations: AST, aspartate aminotransferase; ALT, alanine aminotransferase; CON, control; MOD, model.

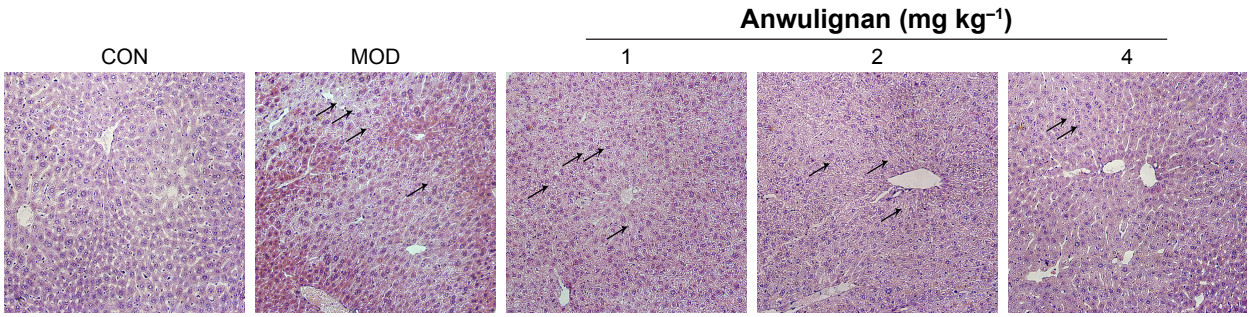

Figure 2 Histopathological changes in the liver of mice (HE ×100).
Notes: The black arrows represented that cytoplasm was loose and vacuolar, the central veins were dilated and congestive, parts of the hepatocytes showed eosinophilic changes.
Abbreviations: CON, control; MOD, model.

staining and the morphological changes in hepatocytes were observed under an optical microscope. As shown in Figure 2, the hepatocytes were normal in morphology, the structure of hepatic lobules was intact, and the central vein and hepatic sinus were normal in the CON group. However, in the MOD group, the hepatocytes were swollen, the cytoplasm was loose and vacuolar, the central veins were dilated and congestive, parts of the hepatocytes showed an eosinophilic change, and there was an accumulation of inflammatory cells around the hepatic lobules, presenting significant damages of the hepatocytes. In comparison to the MOD group, the injuries of hepatocytes were significantly improved in 2 and 4 mg kg^{-1} Anwulignan groups, showing a normal arrangement of cells and no eosinophilic change and inflammatory cell accumulation, while the hepatic injuries were not significantly relieved in 1 mg kg^{-1} Anwulignan group. The above results indicated that D-gal could induce the liver injury in mice and Anwulignan had a significant protective effect against the injury.

Effects of Anwulignan on the oxidative stress in D-gal-treated mice

In order to evaluate the effect of Anwulignan on the oxidative stress in D-gal-treated mice, key biomarkers (SOD, GSH-Px, MDA, and 8-OHdG) in the peripheral blood and livers of mice were detected in this study. As shown in Figure 3A and B, in comparison to the CON group, SOD and GSH-Px activities were significantly reduced in the MOD group ($P<0.01$ and $P<0.05$, respectively). Whereas, in comparison to the MOD group, SOD and GSH-Px activities were significantly increased in 2 and 4 mg kg^{-1} Anwulignan groups ($P<0.01$ and $P<0.05$, respectively), those were not significantly changed in 1 mg kg^{-1} Anwulignan group ($P>0.05$).

As shown in Figure 3C and D, in comparison to the CON group, MDA and 8-OHdG contents were significantly increased in the MOD group ($P<0.01$), whereas, in comparison to the MOD group, MDA and 8-OHdG contents in the peripheral blood and liver tissues of mice were significantly reduced in 1, 2, and 4 mg kg^{-1} Anwulignan groups ($P<0.05$ or $P<0.01$, respectively. But only MDA contents of peripherial blood in 1 mg kg^{-1} Anwulignan group showed no significance). These results showed that Anwulignan has antioxidant activities, which may contribute to its protective effect against hepatic injury induced by D-gal in mice.

Effects of Anwulignan on the gene expression in the liver p38 MAPK–Nrf2–HO-1 pathway in D-gal-treated mice

p38 MAPK–Nrf2–HO-1 pathway plays an important role in regulating the antioxidant damage in the body.[20] In order to investigate the mechanism underlying the antioxidant effects of Anwulignan, the expressions of p38 MAPK, Nrf2, and HO-1 genes in the liver tissue were detected at both mRNA and protein levels. The Reverse Transcription-Polymerase Chain Reaction (RT-PCR) results (Figure 4) showed that in comparison to the CON group, there were no significant differences in the expression levels of p38 MAPK but significant increase in Nrf2 and HO-1 in the MOD group and also in all Anwulignan groups ($P<0.05$ and $P<0.01$, respectively). Furthermore, in comparison to the MOD group, the expressions of HO-1 and Nrf2 were significantly elevated in 2 and 4 mg kg^{-1} Anwulignan groups ($P<0.05$ and $P<0.01$, respectively) but not significant in 1 mg kg^{-1} Anwulignan group ($P>0.05$).

The results of Western blot (Figure 5) were consistent with those of RT-PCR, showing that the expressions of p38 MAPK were not significantly changed, but those of phosphorylated p38 MAPK as well as Nrf2 and HO-1 were increased significantly in all other groups in comparison to CON group ($P<0.05$ and $P<0.01$, respectively), whereas in comparison to the MOD group, the expressions of p38 MAPK phosphorylation, Nrf2, and HO-1 were significantly increased in the liver tissues of mice in 2 and 4 mg kg^{-1} Anwulignan groups ($P<0.01$), suggesting that Anwulignan might play a protective role against the hepatic oxidative damage by activating the p38 MAPK–Nrf2–HO-1 signaling pathway.

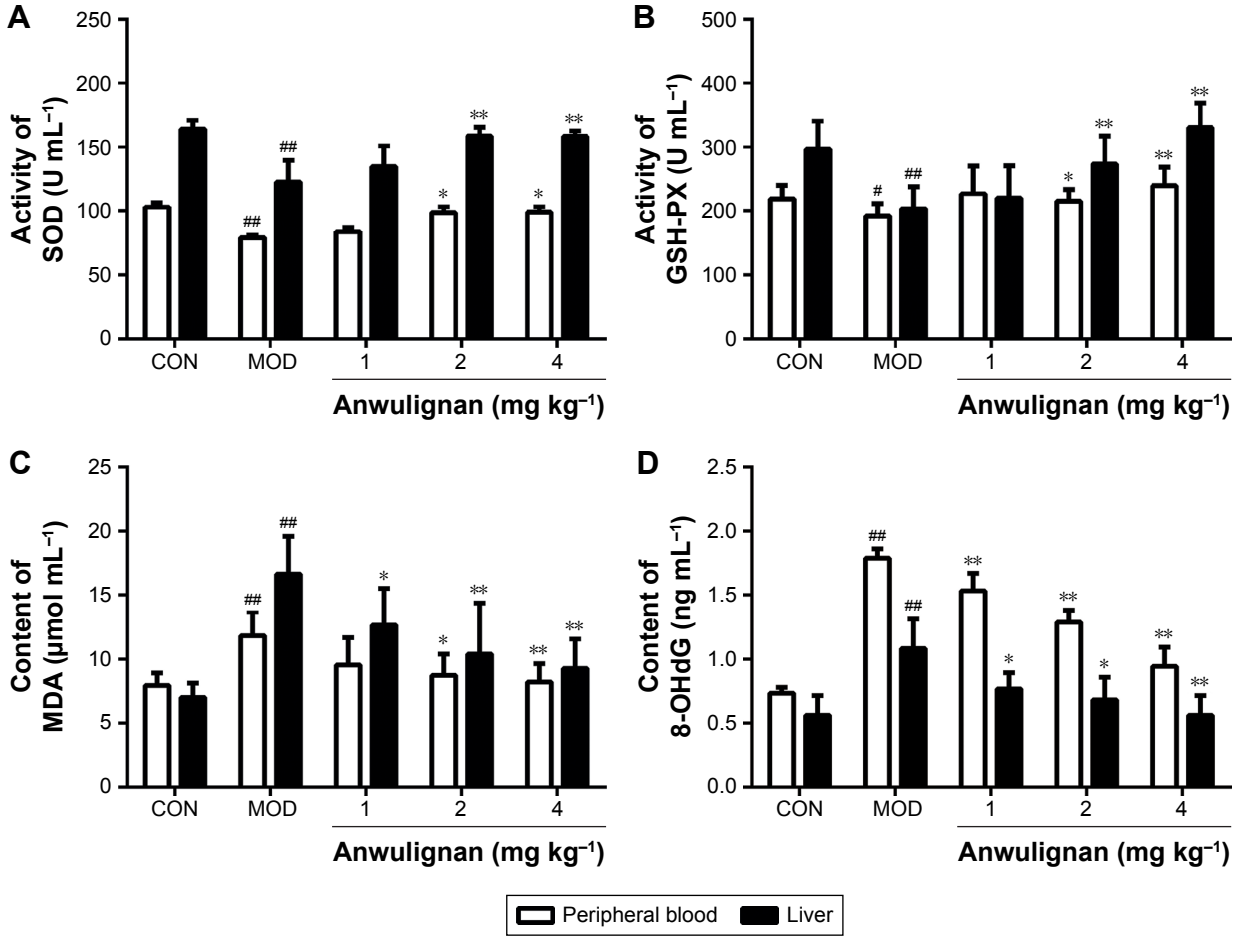

Figure 3 Effects of Anwulignan on SOD and GSH-Px activities and MDA and 8-OHdG contents in the serum and liver tissue of mice (mean ± SD, n=12).
Notes: (**A**) Effects of Anwulignan on SOD activities in the serum and liver tissue. (**B**) Effects of Anwulignan on GSH-Px activities in the serum and liver tissue. (**C**) Effects of Anwulignan on MDA contents in the serum and liver tissue. (**D**) Effects of Anwulignan on 8-OHdG contents in the serum and liver tissue. $^{\#}P<0.05$, compared with the control group; $^{\#\#}P<0.01$, compared with the control group; $^{*}P<0.05$, compared with the model group; $^{**}P<0.01$, compared with the model group.
Abbreviations: GSH-Px, glutathione peroxidase; MDA, malonaldehyde; 8-OHdG, 8-hydroxy-2-deoxyguanosine; SOD, superoxide dismutase; CON, control; MOD, model.

Effects of Anwulignan on the HepG2 cell viability

D-gal could concentration-dependently decrease HepG2 cell viability (<80%) at ≥75 mM, and then, 75 mM of D-gal was selected to induce the injury of liver cells. Anwulignan showed a good dose effect on the cell viability in the range from 0.625 to 1.25 and 2.5 μg mL^{-1}. As shown in Figure 6, in comparison to CON group, the cell viability decreased significantly in the MOD group ($P<0.01$). However, Anwulignan increased the cell viability at 1.25 and 2.5 μg mL^{-1} ($P<0.05$ and $P<0.01$), suggesting that Anwulignan has a protective effect on the D-gal-induced HepG2 cell injury.

Effects of Anwulignan on the apoptosis in the liver

Caspase-3 is the executor of apoptosis, and its content can indicate the apoptosis degree.[21] In order to examine the effect of Anwulignan on apoptosis, the protein content of caspase-3 was detected by ELISA and Western blot. As shown in Figure 7A and B, Western blot results showed that the content of caspase-3 in the MOD group increased significantly ($P<0.01$) in comparison to the CON group, whereas the content of caspase-3 in all Anwulignan groups decreased significantly ($P<0.01$) in comparison to the MOD group. As shown in Figure 7C, the results of ELISA were consistent with Western blot. In comparison to CON group, the content of caspase-3 in the MOD group increased significantly ($P<0.01$). However, in comparison to MOD group, the content of caspase-3 in the 2 and 4 mg kg^{-1} Anwulignan groups decreased significantly ($P<0.05$ or $P<0.01$). These results showed that Anwulignan could inhibit the apoptosis of injured liver cells.

Discussion

S. sphenanthera, a traditional Chinese medicine, was first recorded in the ancient pharmaceutical book *Shennong*

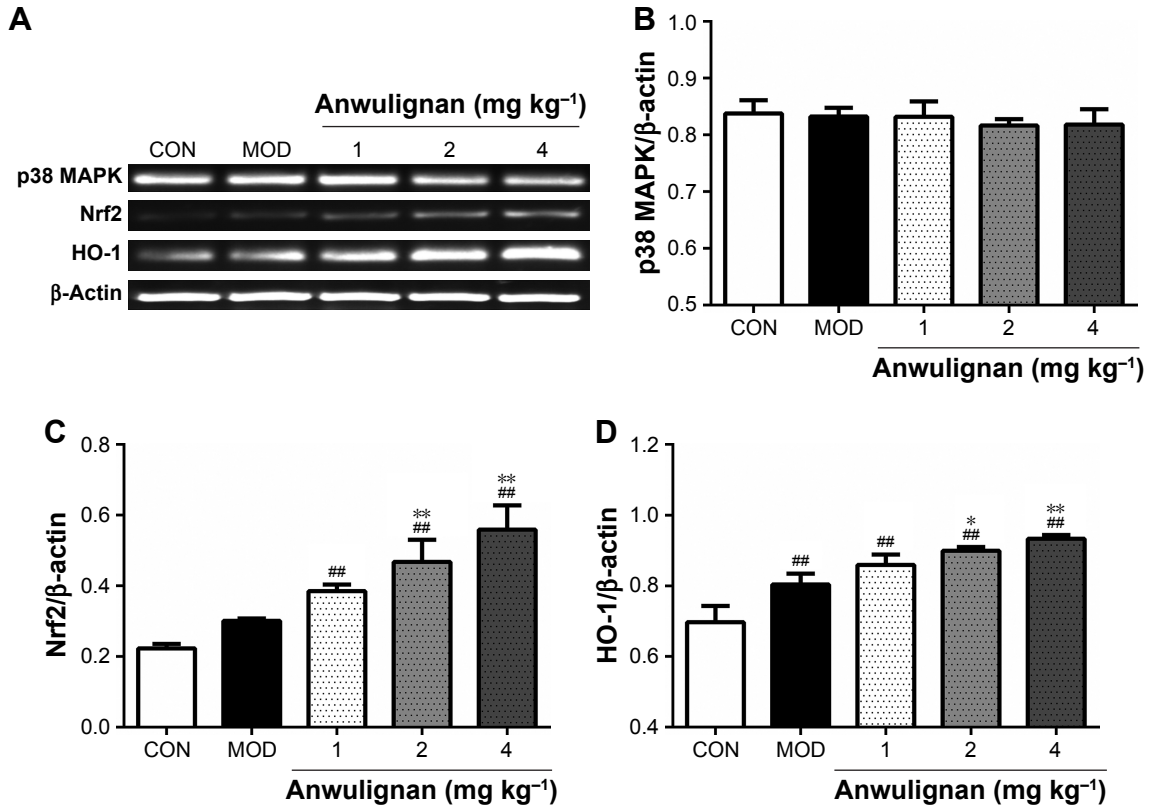

Figure 4 Effects of Anwulignan on the expressions of p38 MAPK, Nrf2, and HO-1 mRNA in the liver tissue of mice (mean ± SD, n=3).
Notes: (**A**) Agarose gel electrophoresis images of p38 MAPK, Nrf2, HO-1, and β-actin by RT-PCR. (**B**) Column charts of p38 MAPK/β-actin by RT-PCR. (**C**) Column charts of Nrf2/β-actin by RT-PCR. (**D**) Column charts of HO-1/β-actin by RT-PCR. $^{\#\#}P<0.01$, compared with the control group; $^{*}P<0.05$, compared with the model group; $^{**}P<0.01$, compared with the model group.
Abbreviations: MAPK, mitogen-activated protein kinase; CON, control; MOD, model; RT-PCR, reverse transcription-polymerase chain reaction.

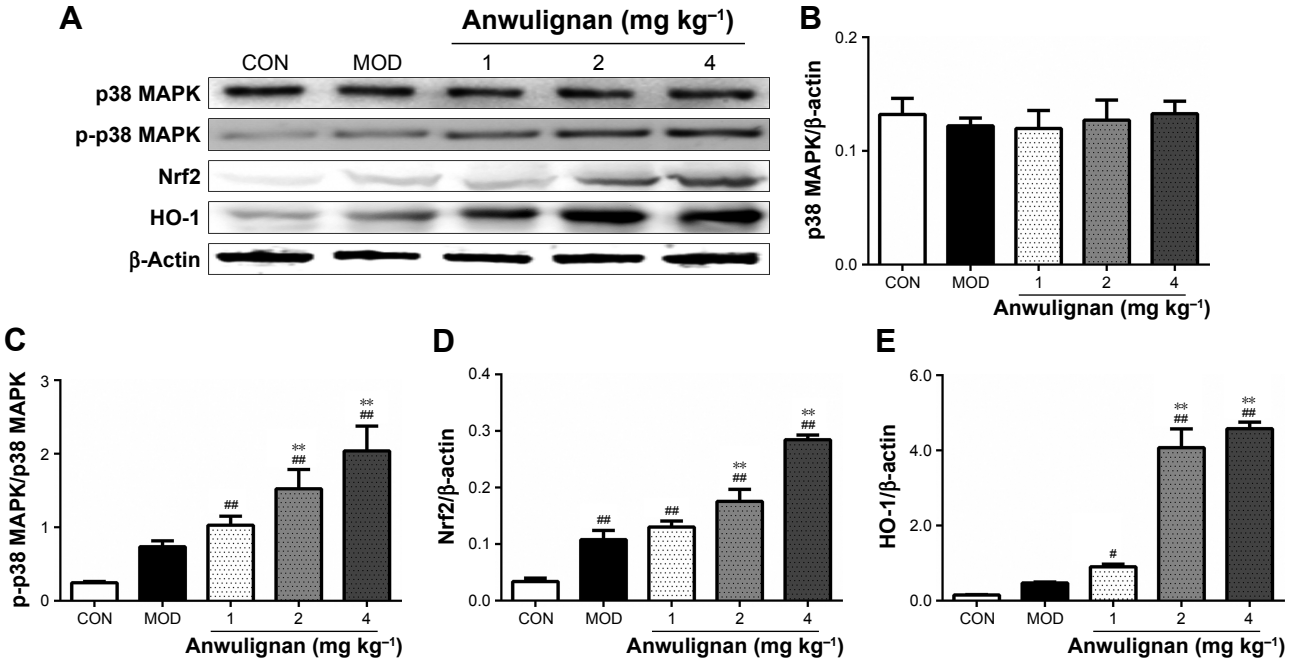

Figure 5 Effects of Anwulignan on the expressions of p38 MAPK, p-p38 MAPK, Nrf2, and HO-1 proteins in the liver tissue of mice (mean ± SD, n=3).
Notes: (**A**) p38 MAPK, p-p38 MAPK, Nrf2, HO-1, and β-actin protein electrophoresis images (Western blotting). (**B**) p38 MAPK/β-actin column charts (Western blotting), (**C**) p-p38 MAPK/p38 MAPK column charts (Western blotting), (**D**) Nrf2/β-actin column charts, and (**E**) HO-1/β-actin column charts (Western blotting). $^{\#}P<0.05$, compared with the control group; $^{\#\#}P<0.01$, compared with the control group; $^{**}P<0.01$, compared with the model group.
Abbreviations: MAPK, mitogen-activated protein kinase; p-p38 MAPK, phosphorylation of p38 MAPK; CON, control; MOD, model.

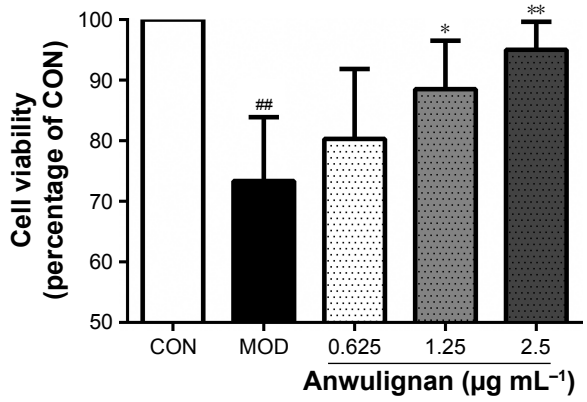

Figure 6 Effects of Anwulignan on HepG2 cell viability.
Notes: ##$P<0.01$, compared with the control group; *$P<0.05$, compared with the model group; **$P<0.01$, compared with the model group.
Abbreviations: CON, control; MOD, model.

Bencaojing as a superior drug and has been used for thousands of years.[22] Modern pharmacological research has demonstrated that *S. sphenanthera* has antioxidant and protective effects against hepatic injuries and most of its biological actions and pharmacological effects can be attributed to the lignan constituents it contains.[23] Anwulignan is a representative composition of *S. sphenanthera*, but there is no report on its antioxidant or protective effects against hepatic injury. Therefore, the present study may be the first try to understand that Anwulignan can contribute to *S. sphenanthera* in the protection of the hepatic injury.

D-gal-induced mouse aging model is often used to observe the aging-caused tissue injuries, behavioral dysfunctions, and molecular changes in the body and the improvements by the interventions. In regard to the mechanism of this model, in brief, a long-time exposure to the oversupply of D-gal, the animals will suffer an accumulation of the galactose and its final metabolite, galactitol. This increased galactitol will cause cell osmotic stress, swelling, and metabolic disorders and dysfunction, damage and consume the antioxidant defense system, and then, result in the accumulation of ROS, such as hydrogen peroxide and superoxide radicals, the decline in antioxidant enzyme activity, and the brain, liver, and other tissues' injuries.[24,25]

Liver index, serum ALT and AST, and histological pathology are main indicators to evaluate liver health.[26,27] D-gal-induced liver injury is considered as a well-established experimental model closely similar to morphological and functional features of liver aging.[2,5,28] In accordance with the relevant reports, the present results showed that in D-gal-treated mice, the decreased liver indexes, the increased serum AST and ALT levels, and the changed histological pathology showed a significant hepatic damage. While these indicators were significantly improved by Anwulignan, suggesting that Anwulignan has a significant protective effect against the D-gal-induced hepatic injury, the effect might be in a dose-dependent manner.

SOD and GSH-Px are the most important antioxidant enzymes in the primary defense system against ROS during oxidative stress.[29–31] Under normal physiological conditions, SOD and GSH-Px efficiently counteract the oxidative damage induced by free radicals. However, they are overwhelmed under excessive oxidative stress conditions. In the present study, the activities of SOD and GSH-Px were

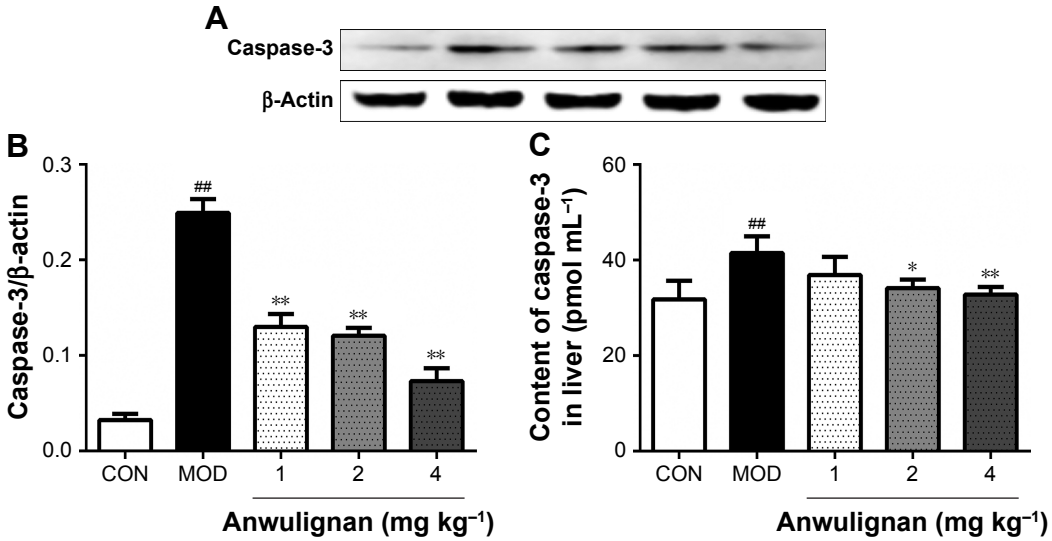

Figure 7 Effects of Anwulignan on the apoptosis in the liver.
Notes: (**A**) Caspase-3 and β-actin protein electrophoresis images (Western blotting). (**B**) Caspase-3/β-actin column charts (Western blotting). (**C**) Effects of Anwulignan on caspase-3 contents in the liver tissue. ##$P<0.01$, compared with the control group; *$P<0.05$, compared with the model group; **$P<0.01$, compared with the model group.
Abbreviations: CON, control; MOD, model.

found to be significantly lower in the liver of D-gal-treated mice than those in the control mice, meanwhile Anwulignan significantly increased their activities. In addition, an increase in ROS levels causes lipid peroxidation and the peroxidation of polyunsaturated fatty acids in biological membranes leads to the formation of MDA; therefore, MDA is used as an indicator of oxidative stress damage.[32,33] The levels of MDA were significantly higher in the liver of D-gal-treated mice, indicating that treatment with D-gal could induce the lipid peroxidation in mice by increasing the production of ROS. Similar findings have been reported in liver and kidney of D-gal-treated mice.[5] Our results showed that Anwulignan significantly reduced the levels of MDA in the liver and serum of mice, indicating that Anwulignan exerted antioxidant effects by preventing ROS-induced lipid peroxidation in D-gal-treated mice. In addition, 8-OHdG is one of the main products of DNA oxidation. The content of 8-OHdG in cells can reflect the degree of oxidative stress.[34] Our results showed that the level of 8-OHdG was significantly reduced in Anwulignan-treated mice, suggesting that Anwulignan could alleviate the DNA damage induced by D-gal. All above results suggest that Anwulignan can counteract the oxidative stress induced by D-gal to play a protective effect against the hepatic injury in mice.

p38 MAPK is a class of MAPKs that are responsive to stress stimuli. Oxidative damage can activate the p-p38 MAPK,[35–38] and then, p-p38 MAPK stimulates Nrf2 dissociated from Keap1. Nrf2 is a basic leucine zipper protein that regulates the expression of antioxidant proteins against oxidative damage triggered by injury and inflammation.[39–42] After the dissociated Nrf2 enters the nucleus, it binds to antioxidative response element and promotes the expression of HO-1. HO-1, the final and key element of this pathway, is an inducible isoform of heme oxygenase, which catalyzes the degradation of heme, producing biliverdin and bilirubin, ferrous iron, and carbon monoxide,[43,44] and they are powerful free radical scavengers in the body.[45,46] Our present results showed that the intracellular p38 MAPK–Nrf2–HO-1 signaling pathway was activated by not only Anwulignan but also D-gal. In fact, D-gal, as an oxidative stress stimulus, can activate the increase in p38 MAPK and its downstream products. However, we speculated that the beneficial effects from the activation of p-p38 MAPK, Nrf2, and HO-1 by D-gal could not overcome its harmful effects from the accumulation of galactitol, which can increase the accumulation of ROS, whereas Anwulignan, through the p-p38 MAPK and up-regulation of the expression of downstream Nrf2 and HO-1, and antioxidative effects might play the protective role against the oxidative damage, finally protecting the liver from the injury induced by D-gal.

Caspases are protease family that play an important role in the process of cell death (including apoptosis and necrosis) and inflammation. Caspase-3 plays an irreplaceable role in cell apoptosis. Activated caspase-3 can break down DNA into nucleosomes and cause apoptosis.[47] Our results showed that the D-gal increased caspase-3 content in mice liver significantly. However, Anwulignan can significantly decrease the content of caspase-3, indicating that the Anwulignan has a significant protective effect on liver cell apoptosis induced by D-gal.

Conclusion

This study found that Anwulignan had the protective effect against the oxidative hepatic injury induced by D-gal in mice, which may be associated with the activation of p38 MAPK–Nrf2–HO-1, increases the injured cell viability, and decreases caspase-3 contents in liver. This study may provide a theoretical basis for the development of drugs and health food for the improvement in the hepatic injury and liver aging.

Acknowledgments

We thank all our colleagues working at the Jilin *Schisandra* Development and Industrialization Engineering Research Center. This study is financially supported by Grants from Jilin Provincial Science and Technology Department (201603103YY, 20162004, 20170309006YY, and 20150311047YY) and Jilin City Bureau of Science and Technology (20166018, 20163024, 20163054, and 20162004).

Disclosure

The authors report no conflicts of interest in this work.

References

1. Go YM, Jones DP. Redox theory of aging: implications for health and disease. *Clin Sci*. 2017;131(14):1669.
2. Huandong Z, Li Jian ZJ, et al. Antioxidant effects of compound walnut oil capsule in mice aging model induced by D-galactose. *Food & Nutrition Research*. 2018;62(4):20.
3. Anantharaju A, Feller A, Chedid A. Aging liver. A review. *Gerontology*. 2002;48(6):343–353.
4. Fan SH, Zhang ZF, Zheng YL, Lu J, et al. Troxerutin protects the mouse kidney from d-galactose-caused injury through anti-inflammation and anti-oxidation. *Int Immunopharmacol*. 2009;9(1):91–96.
5. Feng Y, Yu YH, Wang ST, et al. Chlorogenic acid protects D-galactose-induced liver and kidney injury via antioxidation and anti-inflammation effects in mice. *Pharm Biol*. 2016;54(6):1027–1034.
6. Zhang H, Jiang Y, Wu J, et al. Metabolic mapping of *Schisandra sphenanthera* extract and its active lignans using a metabolomic approach based on ultra high performance liquid chromatography with high-resolution mass spectrometry. *J Sep Sci*. 2017;40(2):574–586.

7. Wang YH, Gao JP, Chen DF. Determination of lignans of Schisandra medicinal plants by HPLC. *Zhongguo Zhong Yao Za Zhi*. 2003;28(12):1155–1160.
8. Gao JP, Wang YH, Yu QY, et al. Determination by HPLC and variation regularity of lignan constituents in Chinese crude drug fructus schisandrae sphenantherae. *Chinese Journal of Natural Medicines*. 2003;1:89–93.
9. Xu M, Wang G, Xie H, et al. Determination of schizandrin in rat plasma by high-performance liquid chromatography-mass spectrometry and its application in rat pharmacokinetic studies. *J Chromatogr B Analyt Technol Biomed Life Sci*. 2005;828(1–2):55–61.
10. Wang GP, Zhang ZC, Xia CM. Efficacy of pentaester tablets in treatment of alcoholic hepatitis. *Chinese Medicine and Clinical*. 2013;31(8):467–469.
11. Fx F. Five ester tablets prevent liver damage caused by pulmonary tuberculosis in 110 cases. *Henan Traditional Chinese Medicine*. 2014;34(9):1711–1712.
12. Xiao WL, Huang SX, Wang RR, et al. Nortriterpenoids and lignans from *Schisandra sphenanthera*. *Phytochemistry*. 2008;69(16):2862–2866.
13. Jiang SJ, Wang YH, Sphenanlignan CDF. A new lignan from the seeds of *Schisandra sphenanthera*. *Chinese Journal of Natural Medicines*. 2005;3(2):78–82.
14. Jiang SL, Zhang YY, Chen DF. Effects of heteroclitin D, schisanhenol and (+)-anwulignan on platelet aggregation. *Journal of Shanghai Medica*. 2005;32(4):467–470.
15. Wei H, Sun L, Tai Z, et al. A simple and sensitive HPLC method for the simultaneous determination of eight bioactive components and fingerprint analysis of *Schisandra sphenanthera*. *Anal Chim Acta*. 2010;662(1):97–104.
16. Liu JS. The isolation and structure of (+)-Anwulignan. *Chinese Journal of Organic Chemistry*. 1988;03:227–228.
17. Deng Y, Zhang Y, Zhang R, et al. Mice in vivo toxicity studies for monohaloacetamides emerging disinfection byproducts based on metabolomic methods. *Environ Sci Technol*. 2014;48(14):8212–8218.
18. Kim HC, Nam CM, Jee SH, et al. Normal serum aminotransferase concentration and risk of mortality from liver diseases: prospective cohort study. *BMJ*. 2004;328(7446):983–986.
19. Williams AL, Hoofnagle JH. Ratio of serum aspartate to alanine aminotransferase in chronic hepatitis. Relationship to cirrhosis. *Gastroenterology*. 1988;95(3):734–739.
20. Wong SY, Tan MG, Wong PT, Herr DR, Lai MK. Andrographolide induces Nrf2 and heme oxygenase 1 in astrocytes by activating p38 MAPK and ERK. *J Neuroinflammation*. 2016;13(1):251.
21. Harrington HA, Ho KL, Ghosh S, Tung KC. Construction and analysis of a modular model of caspase activation in apoptosis. *Theor Biol Med Model*. 2008;55(11):26–26.
22. Lu Y, Chen DF. Analysis of Schisandra chinensis and *Schisandra sphenanthera*. *J Chromatogr A*. 2009;1216(11):1980–1990.
23. Yu CY, Yu CR, Li H. Schisandra total lignin attenuates apoptosis of endoplasmic reticulum pathway to delay mouse brain aging. *Chinese Journal of Pathophysiology*. 2014;11(30):1967–1973.
24. Yang YC, Lin HY, Su KY, et al. Rutin, a flavonoid that is a main component of saussurea involucrata, attenuates the senescence effect in D-Galactose aging mouse model. *Evidence-Based Complementray and Alternative Medicine*. (2012-8-16), 2012, 2012;2012(4):980276.
25. He M, Zhao L, Wei MJ, et al. Neuroprotective effects of (−)-epigallocatechin-3-gallate on aging mice induced by D-galactose. *Biol Pharm Bull*. 2009;32(1):55–60.
26. Zhuang Y, Ma Q, Guo Y, Sun L. Protective effects of rambutan (Nephelium lappaceum) peel phenolics on H_2O_2-induced oxidative damages in $HepG_2$ cells and d-galactose-induced aging mice. *Food Chem Toxicol*. 2017;108(Pt B):554–562.
27. Xu LQ, Xie YL, Gui SH, et al. Polydatin attenuates d-galactose-induced liver and brain damage through its anti-oxidative, anti-inflammatory and anti-apoptotic effects in mice. *Food Funct*. 2016;7(11):4545.
28. Yu Y, Bai F, Liu Y, et al. Fibroblast growth factor (FGF21) protects mouse liver against D-galactose-induced oxidative stress and apoptosis via activating Nrf2 and PI3K/Akt pathways. *Mol Cell Biochem*. 2015;403(1–2):287–299.
29. Dong L, He YZ, Wang YL, et al. Research progress on application of superoxide dismutase (SOD). *Journal of Agricultural Science & Technology*. 2013;15(5):53–58.
30. Fuxing D, Shuang W, Yiwen W, et al. Quercetin ameliorates learning and memory via the Nrf2-ARE signaling pathway in d-galactose-induced neurotoxicity in mice. *Biochemical and Biophysical Research Communication*. 2017;491(3):636–641.
31. Kaviani E, Rahmani M, Kaeidi A, et al. Protective effect of atorvastatin on d-galactose-induced aging model in mice. *Behav Brain Res*. 2017;334(334):55–60.
32. Hosseini M, Anaeigoudari A, Beheshti F, et al. Protective effect against brain tissues oxidative damage as a possible mechanism for beneficial effects of L-arginine on lipopolysaccharide induced memory impairment in rats. *Drug & Chemical Toxicology*. 2017;22:1–7.
33. Jetawattana S. Malondialdehyde (MDA), a lipid oxidation product. *Free Radicals in Biology and Medicine*. 2005;22(77/2):9–18.
34. Valavanidis A, Vlachogianni T, Fiotakis C. 8-hydroxy-2′-deoxyguanosine (8-OHdG): A Critical Biomarker of Oxidative Stress and Carcinogenesis. *Journal of Environmental Science and Health, Part C*. 2009;27(2):120–139.
35. Zarubin T, Han J. Activation and signaling of the p38 MAP kinase pathway. *Cell Res*. 2005;15(1):11–18.
36. Cuadrado A, Nebreda AR. Mechanisms and functions of p38 MAPK signalling. [Review] [172 refs]. *Biochemical Journal*. 2010;429(3):403–417.
37. Raingeaud J, Gupta S, Rogers JS, et al. Pro-inflammatory cytokines and environmental stress cause p38 mitogen-activated protein kinase activation by dual phosphorylation on tyrosine and threonine. *J Biol Chem*. 1995;270(13):7420–7426.
38. Ono K, Han J. The p38 signal transduction pathway: activation and function. *Cell Signal*. 2000;12(1):1–13.
39. Jaiswal AK. Nrf2 signaling in coordinated activation of antioxidant gene expression. *Free Radic Biol Med*. 2004;36(10):1199–1207.
40. Kaspar JW, Niture SK, Jaiswal AK. Nrf2:INrf2 (Keap1) signaling in oxidative stress. *Free Radic Biol Med*. 2009;47(9):1304–1309.
41. Truyen N, Paul N, Pickett CB. The Nrf2-Antioxidant response element signaling pathway and its activation by oxidative stress*. *Journal of Biological Chemistry*. 2010;284(20):13291–13295.
42. Gold R, Kappos L, Arnold DL, et al. Placebo-controlled phase 3 study of oral BG-12 for relapsing multiple sclerosis. *N Engl J Med*. 2012;3672(12):1098–1107.
43. Kikuchi G, Yoshida T, Noguchi M. Heme oxygenase and heme degradation. *Biochem Biophys Res Commun*. 2005;338(1):558–567.
44. Ryter SW, Alam J, Choi AM. Heme oxygenase-1/carbon monoxide: from basic science to therapeutic applications. *Physiol Rev*. 2006;86(2):583–650.
45. Kozakowska M, Dulak J, Józkowicz A. Heme oxygenase-1 – more than the cytoprotection. *Postepy Biochem*. 2015;61(2):147–158.
46. Suttner DM, Dennery PA. Reversal of HO-1 related cytoprotection with increased expression is due to reactive iron. *The FASEB Journal*. 1999;13(13):1800–1809.
47. Perry DK, Smyth MJ, Stennicke HR, et al. Zinc is a potent inhibitor of the apoptotic protease, caspase-3. A novel target for zinc in the inhibition of apoptosis. *J Biol Chem*. 1997;272(30):18530–18533.